Mansoura Journal for Computer and Information Sciences (2024), Vol.**19**, No.**1**
doi:10.21608/mjcis.2024.312462.1006

Mansoura Journal for Computer and Information Sciences

ARTICLE

Lung Cancer Detection Using Hybrid Convolution Neural Network and Recurrent Neural Network

Omnia Alaa,* Muhammad H. Zayyan, Mohammed Alrahmawy, and Samir Elmougy

Department of Computer Science, Faculty of Computers and Information Sciences, Mansoura, Egypt
*Corresponding author: omniaalaa@mans.edu.eg

(Received: 17 August 2024; Accepted: 26 October 2024; Published: 28 October 2024)

Abstract

Humans are susceptible to the common and serious disease known as cancer. Lung Cancer (LC) is considered these days as the most common form of cancer in many nations. In this paper, we developed a five-stage method for detecting lung cancer in CT images, which includes preprocessing the image with a Wiener filter, segmenting the image using global thresholding, feature extraction, feature selection, and classification. Statistical and morphological data are combined to create a gray-level-co-occurrence matrix (GLCM), which is used to extract textural features during the feature extraction step. To extract deep features, hybrid Convolution Neural Networks (CNN) and Recurrent Neural Networks (RNN) are also employed. The Slime Mould Algorithm (SMA) is then used to choose the best features using a wrapper method fitness function that considers the criterion's correctness. The classification techniques are then used. Using 100 samples of lung CT images as a sub-dataset, the suggested method is assessed. The experiment results show that SMA is the best feature selection algorithm among other used algorithms, in which it reaches a 95% accuracy rate, based on Lung Image Database Consortium Image Collection (LIDC-IDRI). This dataset includes 1018 images of malignant and healthy tissue. Moreover, Residual Neural Network (ResNet 18) is shown to be the best classification technique among other used techniques, reaching 98.5% accuracy, 98.5% sensitivity, and 99.5% specificity.

Keywords: Artificial intelligence; lung cancer detection; deep learning ; image processing; image classification.

1. Introduction

Currently thought to be the most common and fatal disease affecting humans is cancer. In the world, millions of people die from cancer every year, according to the World Health Organization (WHO) [1]. Humans can develop many different types of cancer; some are fatal, while others are treatable. These days, common cancers like liver, lung, and breast cancer are becoming more prevalent [2].

One of the highest cancer types that cause fatalities in Egypt is lung cancer disease (LCD) which is sometimes considered the most prevalent type of cancer worldwide [3]. It is critical to accurately and promptly identify cancer in its early stages to save human lives [4]. To lower the risk of lung tumor disease-related death, early detection of lung tumors is essential. Due to the rapid metastasis of lung cancer to the brain, liver, bones, and adrenal glands, early detection of lung cancer is crucial [4]. Because of these factors, many research works have proposed effective methods for categorizing LCDs.

Magnetic Resonance Imaging (MRI), Computed Tomography (CT) scans, and X-rays are among the imaging methods used to detect lung cancer [5]. Since CT scans provide a three-dimensional view of the lungs and the tissues that overlap in chest radiographs, several procedures rely on them for image capture [5]. The way that different body parts absorb X-rays is examined by CT imaging. Its great resolution allows it to capture the human skeleton. A technique utilized in MRI imaging is nuclear magnetic resonance. Although it can gather human body soft tissue information, its resolution is inadequate [6]. These findings demonstrate how challenging and time-consuming lung cancer detection is.

Artificial Intelligence (AI) has proved extremely successful in the medical domain. This involves using image analysis and Machine Learning (ML) techniques in medicine to identify, diagnose, and categorize illnesses. The goal of ML is to develop models and algorithms that can adapt and learn from large datasets. Based on historical data and trends, ML algorithms can forecast and decide by using this data. Large datasets can be analyzed by ML algorithms, which are made to pull out important information [7]. Due to its capacity to extract high-level features even from raw data over massive data to obtain an input space representation, Deep Learning (DL) demonstrated its better performance, particularly accuracy[8]. In therapy planning, LC diagnosis, classification, and prediction are essential. Therefore, the purpose of this paper is to develop an AI and image processing-based system for LCD detection to identify benign or malignant changes in CT scans. Specifically, we improve the architecture described in [3] and use AI techniques to provide a novel LC detection method using the Image Collection of the Lung Image Database Consortium (LIDC-IDRI). The following points highlight our main contributions:

- Creating a method to identify lung cancer at an earlier stage.
- Combining textural features using GLCM and deep features using hybrid CNN and RNN to increase accuracy of classification.
- Utilizing the Slime Mould Algorithm (SMA) in the feature selection stage.
- Using Residual neural network (ResNet-18) for the classification stage.

The remaining portion of this research is written as follows. Section 2 introduces the Literature review of this paper. Section 3 introduces the suggested technique. Section 4 discusses the experimental outcomes. Section 5 concludes with the conclusion and future work.

2. Literature Reivew

Finding lung cancer nodules was an essential task in creating a Computer-Aided Diagnosis (CAD) system for the disease's detection [9]. As a result, numerous researchers plan to create various techniques for identifying and categorizing LC.

Silva et al [10] suggested a CAD method based on the ResNet-34 and U-Net designs. They used four distinct cross-cohort datasets to test the approach. The dice similarity coefficient (DSC) was employed by the authors to assess the efficacy of their methodology. DSC, which has a value between 0 and 1, is a frequently used statistic in medical picture segmentation tasks that assesses the

overlap between the expected and ground truth segmentation. When the expected and ground truth segmentation perfectly match, the DSC value is 1. Across the four distinct cross-cohort datasets, the CAD technique produced a mean DSC value greater than 0.93. This implies that the technique was successful in precisely identifying and segmenting structures of interest within the medical imaging data. After reviewing the procedure, two radiation specialists found several drawbacks, especially with consolidation. Still, the devised method produced an F-score of 99.2% and an accuracy of over 99.3%. To assess the illness, the study used four performance measures. Furthermore, two DL techniques were used to assess the system on three datasets.

Alsheikhy et al [11] constructed a manual process machine to identify lung cancer. It used a Gabor filter and many CT scans. In the collection, 1,800 images—or 900 out of the total—showcase children who had received a lung cancer diagnosis. The dataset was gathered from the Integrated Modules for Bioassay Analysis (IMBA) Home Database, with each image having a resolution of 200 × 200 pixels. At 99.42% on average and 99.61% at maximum accuracy, this CAD system performs smoothly. Recall, precision, and F-score all reach remarkable highs of 99.76%, 99.88%, and 99.82%, respectively. Also, the system performs admirably on other critical performance parameters. Faruqui et al [12] implemented a deep-CNN-based model intended to improve lung cancer CAD's accuracy. To enhance diagnostic capabilities, it blends wearable sensor-based medical IoT (MIoT) data with CT-scan images. By extracting information from both data sets, Lung-Net's unique 22-layer CNN architecture achieves a low False Positive (FP) rate of 3.35% and a high accuracy of 96.81% when classifying lung cancer into five groups. It performs better than comparable CNN-based classifiers. Additionally, LungNet has a 91.6% accuracy rate and a 7.25% false positive rate when classifying stage-1 and stage-2 lung tumors into subclasses. LungNet is a centralized server that runs on a balanced dataset of 525,000 photos for training. Its substage classification, low false positive rate, and excellent accuracy make it a viable option for autonomous lung cancer diagnosis systems.

Shimazaki et al. [13] created and verified a deep-learning model to identify LCD from chest radiographs using adapted CNN architecture with a segmentation method. While the test dataset contained 151 radiographs with 159 nodules/masses, the training dataset comprised 629 radiographs with 652 nodules/masses. The model attained a sensitivity of 0.73 and a mean false positive indication per picture (mFPI) of 0.13 in the independent test dataset. However, when it came to lung tumors that overlapped blind regions as opposed to nonoverlapped locations, the model's sensitivity was lower. For malignant lesions, the average value of the dice coefficient, which gauges how similar the ground truth and predicted masks are, was 0.52. This suggests that the model performed rather well in distinguishing malignant lesions. The low MFPI suggests that, despite these drawbacks, the DL-based model showed promise in identifying lung tumors on chest radiographs with low FP rates. To improve the dice coefficient for malignant lesions and to increase the sensitivity of the model, especially for lung tumors that overlap with blind areas, more investigation and development may be needed.

Hasan et al [14] applied histogram equalization to improve the image. The second stage involved segmenting the images using a watershed algorithm based on markers. With an accuracy of about 72.2%, the assessment was carried out using a dataset of 198 photos that were obtained from the Kaggle website. By contrast, the method discussed in this paper produces a far better accuracy of 99.42%. Additionally, this study's suggested method achieves remarkable results, with recall, precision, and F-scores of 99.76%, 99.88%, and 99.82%, respectively. Bansal et al [15] presented a method to increase the effectiveness of picture classification by combining deep features produced by VGG19, the DL model, with additional specialized feature extraction methods including Scale Invariant Feature Transform (SIFT), Speeded Up Robust Features (SURF), Oriented Fast and Rotated BRIEF (ORB), and the Shi-Tomasi corner detector algorithm. The features were then combined with different machine-learning algorithms to get a classification. The study's empirical results showed that the Random

Forest (RF) classifier outperformed other classifiers with an accuracy of 93.73% when paired with the cooperative characteristics that were generated using the integrated approach. This implies that employing a blend of DL features and traditional features produces more reliable and accurate results than depending only on one feature extractor.

Toğaçar [16] presented the DL model, in which the DarkNet-19 model served as the basis for the creation of the picture classes. Using the equilibrium and manta-ray foraging optimization strategy, the weak features from the feature set derived from the DarkNet-19 model were chosen to construct the image classes. An ideal feature set was then produced by separating these weak features from the remainder of the feature set. The two optimization strategies that were used to produce the appropriate characteristics were classified using the Support Vector Machine (SVM) technique. A remarkable 99.69% was the classifier's overall performance percentage. The evaluation's findings showed an astounding 99.3% area under the curve (AUC). Additionally, the method showed good recall, accuracy, F-measure, and precision rates, with values as high as 97.1%. Prasad et al [3] recommended a method for dividing and categorizing the lung. They applied two steps to develop this system. Multiple procedures, like preprocessing, feature extraction, feature selection, and classification, are involved in the first stage. The second stage consists of segmenting tumors using the fuzzy k-means approach. For the preprocessing stage, this system employed a wiener filter to eliminate noise. Gray Level Co-occurrence Matrix (GLCM) was utilized to extract textural features while VGG-16 was employed to extract deep features during the feature extraction step. The best features are found by using the crow search optimization method. To train a network to categorize lung CT scans as normal or abnormal, the acquired features are fed to the ANN. 99% sensitivity, 100% specificity, and 96% accuracy were achieved by this system.

Talukder et al [17] suggested a hybrid ensemble feature extraction model for lung cancer detection. The LC25000 dataset was used to test the model on lung datasets. The results of their work showed that a hybrid model could detect lung cancer with astounding accuracy rates of 99.05%. These outcomes show how well the suggested method works for correctly diagnosing lung cancer. The study also showed that the suggested hybrid model much outperformed current models, suggesting that it may find use in clinical settings; this illustrates how employing ensemble models of TL models might improve the diagnostic accuracy of LCD. Humayun et al [18] designed a Deep Neural Network (DNN) to be used in lung cancer CAD. Domain Adaptation (DA) approaches were used in this study to develop the classifier to overcome the issue of data availability in medical image analysis. By comparison with current state-of-the-art investigations, the provided model showed effectiveness, non-invasiveness, and fewer parameters. The accuracy with which the Xception, VGG 19, and VGG 16 models classified the lung tissue nodule data set was especially investigated in this study. The accuracy of these models' classification was demonstrated by these outcomes. According to the research, DNNs, preprocessing methods, and transfer learning can all help in lung cancer diagnosis and detection.

Nibali et al [19] offered a method for utilizing CT scan pictures to identify lung cancer in nodes, hence improving the prediction ability of CAD models. To distinguish between benign and malignant lung nodules, this study employs sophisticated CNN and Residual Neural Network (ResNet) architecture. To address the dearth of publicly available datasets, the study makes use of the LIDC-IDRI dataset. Metrics such as AUC, accuracy, specificity, and precision show good performance of the system. Deep residual learning, curriculum learning, and transfer learning work together to increase nodule classification accuracy, which may have uses in other areas of medical imaging. The accuracy level attained by the system was 89.90%.

Shaffie et al [20] proposed a framework that represents the shape of the nodules by capturing geometric properties and appearance attributes using a Markov-Gifbs random domain model. The retrieved geometric properties are merged with an accurate representation of the observed nodules

by the model. With a precision of 91.20% for nodules, this proposal's estimation—which makes use of publicly available data from the Lung Image Database Consortium—shows promise for the identification of lung cancer. Shanthi et al [21] examined various methods for separating non-nodules from lung cancer nodules. They developed the 3D Convolutional Neural Network Technique to lessen or eliminate false positive predictions. Because nodules come in a variety of sizes, employing a single CNN may lead to false positives. Thus, based on size, they separated the nodules into four categories. Additionally, they have employed four distinct 3D CNN sizes. To improve the findings, they put the four classifiers together. Every CNN is made up of several 3D CNNs with different sizes. Better results were obtained by combining the four classifiers. Each CNN was created using a convolutional layer and a max pooling layer. Rectified Linear Unit (ReLU) is the activation function in this case. The output is finally produced using a fully linked layer in conjunction with a softmax layer. Since the size of nodules varies from 3 mm to 3 cm, the prediction made using only one layer may not be accurate for very small nodules or extremely big values. As a result, they combined the output values from all four CNNs and fed them to a final classifier. The entire model was trained using the LUNA16 dataset. The CT scans from the LIDC-IDRI dataset serve as the basis for LUNA16. They thus observed that the fused classifier's output outperformed that of each of the individual classifiers.

Mohan et al [22] used neural networks C3D and 3D DenseNet to diagnose through CT images. The two-stage methods (two separate neural networks are trained for segmentation and classification) and whole lung 3D pictures were used to apply these neural networks, which were then compared. Over a thousand CT images from patients were used in the Data Science Bowl 2017 dataset. Resampling was used to transform all the CT scans into Household Units (HUs, units used to describe the intensity of x-rays) for pre-processing. In the subsequent stage, all patient photos were filtered using a lung tissue range that eliminates all bones from the image, since HU ranges are unique to tumors (-500). The 3D patient picture was shrunk to 120 x 120 x 120 pixels. The 3D DenseNet model outperforms the 3CD model, with results that are quite similar. According to the results, two-stage methods outperformed neural networks trained on full lung 3D pictures.

Toğaçar et al [23] suggested a method for detecting lung cancer based on CNN. They have collected a total of 100 photos from 69 different patients, 50 of which are malignant and the remaining 50 are not. Augmentation was utilized to obtain a healthy dataset because there were fewer photos. In this investigation, CNNs using AlexNet, LeNet, and VGG-16 architectures were employed. The weights for each training set were updated using the optimization technique of stochastic gradient descent (for VGG-16 and AlexNet). In addition, Root Mean Squared Propagation (RMSProp) and adaptive moment estimation (ADAM) were employed as LeNet optimization techniques. To extract the features, the minimum Redundancy - Maximum Relevance (mRMR) method was applied. Following the CNN designs, certain conventional machine learning models including Linear Regression (LR), Latent Dirichlet Allocation (LDA), SVM, K-Nearest Neighbor (KNN), and Decision Tree (DT) are also employed. By applying Principal Component Analysis, the performance was enhanced. An accuracy of 99.51 was achieved by selecting KNN with CNN & mRMR.

Masood et al [24] suggested a technique that uses CNN-based and IoT techniques to identify early signs of lung cancer. They have presented an IoT system that includes wearable smart devices and certain symptom charts that can be used to determine whether the patient is exhibiting any relevant symptoms and should notify the physician. These patients' CT scans were subsequently fed into the CNN model. A Gabor filter was applied as a preliminary step. The Region of Interest was obtained by applying thresholding. As the primary classification model, Dense Fusion Classmate Network (DFCNet) was employed. Using the LIDC-IDRI dataset, the suggested model produced results with 86.02% accuracy, 83.91% sensitivity, and 80.59% specificity.

Vijh et al [25] presented a hybrid bio-inspired method based on 120 image samples from the NCI LCD

Consortium for recognizing LCD. The method employs whale optimization and adaptive Particle Swarm Optimization (PSO). Preprocessing, segmentation via global thresholding, morphological operation, and feature extraction through GLCM, Gray-level run-length matrix (GLRLM), Histogram-oriented Gradient (HOG), Gray-level dependence matrix (GLDM), and Local binary pattern (LBP) comprise their system's stages. With this technique, 97.1% accuracy, 97% sensitivity, and 98.66% specificity are attained.

Ghaderzadeh et al [26] used The Modified Dense Convolutional Neural Architecture Search Network (NASNet) method to offer a CAD system for COVID-19 to differentiate COVID-19 photos from non-covid-19 images. The recommended model performed detection sensitivity, specificity, and accuracy of 0.999, 0.986, and 0.996, in that order. Carvalho Filho et al [27] identified 50,580 pictures from lung CT scans—14,184 of which were classified as malignant nodules and 36,396 as benign—and utilized CNN to classify the results as benign or malignant. 90.7% sensitivity, 93.47% specificity, and 92.63% accuracy were their findings. Wei et al.[28] established a novel unsupervised spectral clustering method that uses the Local Kernel Regression Model (LKRM) to generate a new Laplacian matrix to distinguish between benign and malignant nodules. Kumari et al [29] suggested a method with five stages. Images from the dataset were gathered in phase one. Phase two involves preprocessing the pictures with the median filter. Then, as fuzzy C-means outperform K-means, they are utilized for picture segmentation. In phase four, features are extracted from images using GLCM. Subsequently, the SVM classifier receives the retrieved features for the classification stage. Their method's accuracy score was 96.7%. Wankhade et al. [30] suggest a cutting-edge technique called Cancer Cell Detection utilizing Hybrid Neural Network (CCDCHNN) for early and precise detection. Deep neural networks are used to extract the features from the CT scan images. To protect the patient from this deadly illness, early cancer cell detection depends critically on the accuracy of feature extraction. To increase diagnosis accuracy, an advanced 3D convolution neural network (3D-CNN) is also used in this study. Table 1 discusses the strengths and weaknesses of all of the related work. Also, Table 2 shows the dataset, methods, and results of all literature reviews.

As previously mentioned, these methods do not address the feature extraction or selection stages, instead concentrating solely on categorization. However, several solutions rely on conventional feature extraction techniques such as Size, Wavelet features, Shape, Surface, Edge, and first-order statistics, which causes time-consuming issues for some of these techniques.

Table 1. Comparison of the strengths and weaknesses of all related work

Ref	Year	Pros	Cons
[10]	2022	gives a thorough analysis of the most current studies conducted to create CAD tools employing computed tomography images for tasks linked to lung cancer.	Depends on lung Cancer and the CAD system. Lack of large dataset.
[11]	2023	enabling the development of an automated, intelligent system that uses two deep learning approaches to accurately detect, identify, and categorize NSCLC and its subtypes.	Large execution time.
[12]	2021	introduce LungNet, a unique hybrid deep-convolutional neural network-based model trained on wearable sensor-based medical IoT (MIoT) data and CT scan data.	Balanced dataset
[13]	2022	created and verified a deep-learning model to identify LCD from chest radiographs using adapted CNN architecture with a segmentation method	Small dataset from a single hospital, A screening cohort may have a greater number of FPs.
[14]	2019	create an algorithm that can reliably identify whether lung cancer exists.	Small dataset

[15]	2021	combining deep features produced by VGG19, the DL model, with additional specialized feature extraction methods including SIFT, SURF, ORB, and the Shi-Tomasi corner detector algorithm	The images in the dataset have low resolution and are noisy
[16]	2021	Used two optimization techniques to provide efficient feature	Large dataset and Specific knowledge is needed.
[3]	2021	The method is strong and efficient in lowering false positives.	The suggested method does not identify juxtapleural, well-circumscribed, vascularized, or pleural tail nodules, nor does it stage malignancy.
[17]	2022	Their system executed brilliantly and surpassed alternative methods	A large dataset and Specific knowledge are needed
[18]	2022	Domain Adaptation (DA) approaches were used in this study to develop the classifier to overcome the issue of data availability in medical image analysis	Small dataset images.
[19]	2017	Improving the prediction ability of CAD models	Time-consuming and lacks segmentation.
[20]	2018	Presented a unique framework for the categorization of lung nodules that includes geometric features and a novel higher-order MGRF to model the nodules' appearance features.	Although it can tell benign nodules from malignant ones, it is unable to tell each type's several categories apart.
[21]	2020	developed the 3D Convolutional Neural Network Technique to lessen or eliminate false positive predictions	The small size of the dataset
[22]	2015	Used PET/CT images	Lack of using deep feature extraction
[23]	2020	Used different deep classifiers to improve performance	The small size of the dataset
[24]	2018	suggested a technique that uses CNN-based and IoT techniques to identify early signs of lung cancer.	employing various datasets and scan parameters to produce FP results when there are malignant nodules
[25]	2020	suggested a hybrid bio-inspired algorithm that combines the advantages of adaptive particle swarm optimization (APSO) with work of work of WOA.	The suggested approach restricts its applicability to three-dimensional medical imaging.
[26]	2021	used the NASNet method to offer a CAD system for COVID-19 to differentiate COVID-19 photos from non-covid-19 images	Small images in local dataset
[27]	2018	offered a system for dividing lung nodules into benign and malignant categories.	Time time-consuming for classification due to many features
[28]	2018	An innovative approach for unsupervised spectral clustering was introduced to differentiate between benign and malignant nodules.	using the lung nodule that the radiologists have removed, which is precise but not automatic
[29]	2019	Suggested a method with five stages for classifying cancer images from not.	Lack of selecting optimal features from all features extracted.
[30]	2023	suggest a cutting-edge technique called Cancer Cell Detection utilizing Hybrid Neural Network (CCD-CHNN) for early and precise detection	acquiring enough high-quality training data and enhancing DL models' readability.

Table 2. Comparison of the dataset, methods and results of all related work

Ref	Dataset	Method	Result
[10]	four distinct cross-cohort datasets	ResNet-34 and U-Net designs	F-Score=99.2 Acc over 99.3
[11]	Chest CT Scan, LUNA-16, and LIDC-IDRI	DCNN, VGG-19, LSTM, PCA	ACC=98.8 Recall=99.76 Precision=99.88 F-score=99.82
[12]	LIDC-IDRI, LUNGx	CAD system with deep CNN	ACC=96.81
[13]	dataset collected separately from January 2006 to June 2018 at Their hospital	CNN with segmentation methods	Sensitivity=73 mFP=0.13

[14]	Bowl 2017	marker-controlled watershed segmentation, Linear regression, Logistic regression, KNN, SVM, and RF	ACC=72.2
[15]	dataset Caltech-101	SIFT, SURF, ORB, VGG-19, RF	ACC=93.73
[16]	Dataset with four five classes: two for colon cancer and three for lung cancer	DarkNet-19 and SVM	LAcc, recall, F-score, precision as high as 97.1
[3]	LIDC-IDRI	ANN, SVM, Fuzzy k-means, and crow search optimization	Acc=96 Sensitivity=99 Specificity=100
[17]	LC25000	VGG16, VGG19, DenseNet169, DenseNet201, RF, SVM, LR.	Acc=99.05
[18]	Iraq-Oncology Teaching Hospital/ National center for cancer (IQ-OTH/NCCD)	VGG-16, VGG-19, CNN, Transfer learning (TL)	ACC=98.83 for VGG-16
[19]	LIDC-IDRI	ResNet, multilayer perceptron (MLP)	ACC=89.9
[20]	LIDC-IDRI	Markov-Gifbs random domain model, feed-forward neural network	Precision=91.2 Acc=91.2
[21]	cancer genome atlas (TCGA) dataset	3D CNN, GLCM, stochastic diffusion search (SDS)	ACC for SDS-NN by 2.51%
[22]	Bowl 2017 dataset	FCM, 3D DenseNet, CLAHE	ACC=92.67
[23]	Dataset of 69 patients with 100 images	CNN, AlexNet, LeNet, and VGG-16, RMSProp and ADAM, LR, LDA, SVM, KNN, and DT	ACC=99.51
[24]	LIDC-IDRI	Gabor filter, DFCNet, FCNN	ACC=86.02 Sensitivity=83.91 Specificity=80.59
[25]	NCI LCD Consortium	PSO, WOA, GLCM, GLRLM, HOG, GLDM, and LBP	ACC=97.1 Sensitivity=97 Specificity=98.66.
[26]	A local data set, comprising 10,153 computed tomography scans of 190 patients with and 59 without COVID-19 was used	CNN, NASNet	ACC=0.996 Sensitivity=0.999 Specificity=0.986
[27]	LIDC-IDRI	CNN, Otsu algorithm	ACC=92.63 Sensitivity=90.7 Specificity=93.47
[28]	LIDC-IDRI	LKRM, LR	ACC=85.4
[29]	100 images collected from Kaggle	Median filter, GLCM, Fuzzy C-means, SVM	ACC=96.7
[30]	LIDC-IDRI	3D-CNN, RNN, U-Net	ACC=95% Sensitivity=87% Specificity=90%

3. Method

Our suggested method is covered in this section, where the suggested framework is displayed in Figure 1. for detecting LCD for CT images. Figure 1 illustrates the five steps that make up this method. We Will show the detailed framework in Figure 8

3.1 The used dataset

This work uses 100 LIDC-IDRI dataset lung CT imaging samples as used in [31]. The 1018 cases in this data set comprise thick-sliced medical lung CT scan pictures, with each image varying in thickness from 0.6 to 5 mm. Each case also includes an accompanying XML file including the results of a staged image annotation approach performed by four experienced thoracic radiologists [31]. Radiologists divided lesions into three categories: non-nodule >=3mm, nodule 3 mm, and nodule >=3 mm [3]. In the dataset utilized, an example of a CT image is displayed in Figure 2 [31].

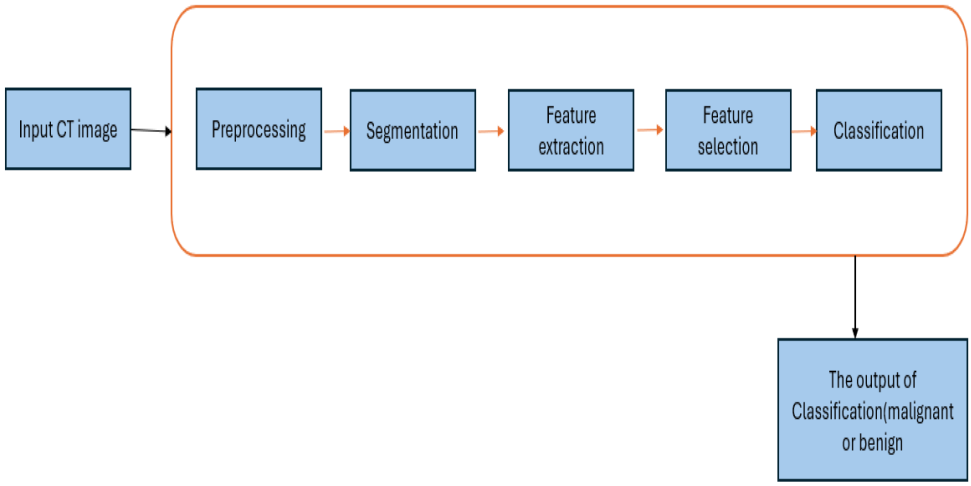

Figure 1. The high level of the overall steps of the proposed technique

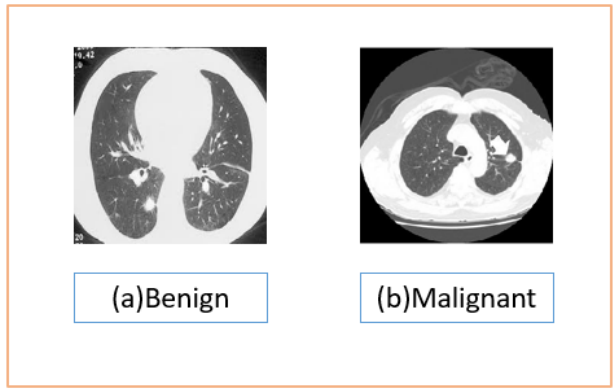

Figure 2. Examples of LIDC-IDRI dataset of two classes (malignant and benign)

3.2 Stages of Framework

3.2.1 Image preprocessing

CT image preprocessing is the first step in the recommended method for reducing noise and enhancing image quality. At this point, the input CT picture has been normalized and converted to grayscale. After that, a wiener filter is used to improve the final image by eliminating noise. In terms of mathematics, the Wiener filter is described as [3]:

$$W(d1, d2) = \frac{H * (d1,\ d2)B_{xx}(d1,\ d2)}{|H(d1,\ d2)|^2 B_{xx}(d1,\ d2) + B_{\eta\eta}(d1,\ d2)} \tag{1}$$

where the power spectrum of CT image and noise are represented by $B_{xx}(d1,\ d2)$, $B_{\eta\eta}(d1,\ d2)$, and $H(d1,\ d2)$ is the burring filter. The Wiener filter is employed as a low pass and inverse filter to eliminate noise and maintain an edge [3].

3.2.2 Image Segmentation

At this point, the image is separated into segments, each consisting of a distinct set of pixels. The global thresholding technique is the most often used segmentation method. For the threshold (T), this method depends on the grayscale pixel's brightness. Using Otsu's threshold, lung sections are segmented from lung CT scans at this stage [27]. Applying Otsu's threshold to the pixel value of an image t(a, b) yields the segmented picture H (a, b). Otsu's method uses a single intensity threshold to separate pixels into two classes: background and foreground [32]. This approach sets a threshold value by utilizing a minimum or maximum inter-class variance. Using the following formula, the Otsu's threshold is determined as [27]

$$H(a,b) = \begin{cases} 1 & if\ t(a,b) < T \\ 0 & if\ t(a,b) \geq T \end{cases} \tag{2}$$

3.2.3 Feature Extraction

Using GLCM, the textural features are initially retrieved from the segmented CT image in this step [29]. Standard deviation, total variance, difference entropy, mean, and other statistical and morphological data are combined to generate GLCM. Next, the segmented CT image is processed by hybrid CNN and RNN to extract deep features. CNNs are feedforward neural networks that use convolutional structures to acquire information about features in the input[33] . In contrast to conventional techniques, CNNs automatically identify and learn from the data, eliminating the need for human feature extraction [34]. The convolutional layer, pooling layer, and fully connected layer are the three main parts of CNNs [35]. The pre-trained CNN network Alexnet is used in this investigation which is shown in Figure3 [36]. Afterward, the features are also taken out of RNN. One family of DL models that can capture sequential dependencies is the RNN class; these models include internal memory. RNNs consider the temporal order of inputs, in contrast to typical NNs that treat inputs as independent entities, which makes them appropriate for tasks involving sequential information [37]. Specific issues in diverse applications have led to the development of numerous types of RNN models, including Long Short-Term Memory (LSTM), bidirectional LSTM, Gated Recurrent Unit (GRU), and bidirectional GRU. In this paper, we used LSTM shown in Figure4 which is an enhanced version of RNN. LSTM models are more successful in retaining and applying information across longer sequences when compared to standard RNNs [38]. Next, we integrated the features that were taken from CNN and RNN. After completing this action, the textural features and deep features are combined to get a matrix of all features for CT images to pass to the next step.

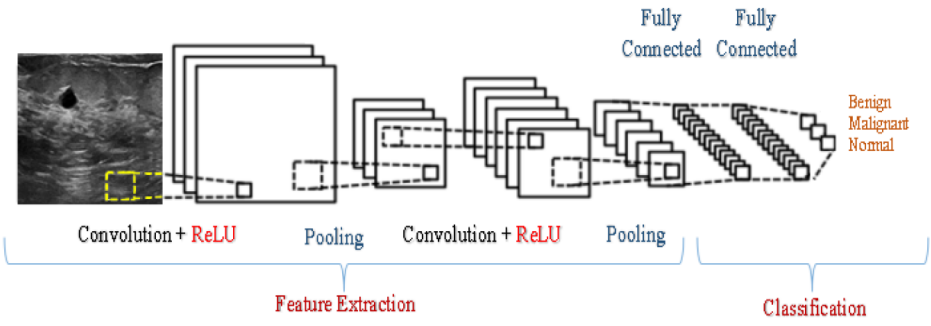

Figure 3. The architecture of Alexnet with CNN architecture [36]

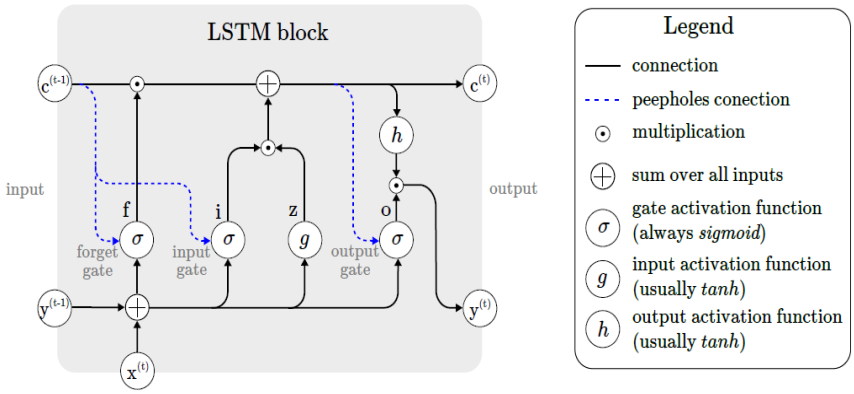

Figure 4. The architecture of LSTM

3.2.4 Feature Selection

The goal of this phase is to reduce computing costs and improve the efficiency of the classification step by extracting important features and ignoring the remainder. To extract the characteristics from the early stage, we applied three classifiers PSO, SMA, and WOA optimization techniques. The wrapping approach is used as a function of fitness that relies on the K-Nearest Neighbor (KNN) algorithm with accuracy criteria utilizing Eq. 3 to choose the best features. For the fitness function, this method uses two parameters (alpha and beta), with values of 0.99 and 0.01 correspondingly. By comparing the accuracy of three optimization algorithms, we saw that SMA is the best with 95% accuracy. The number of features the three optimization methods reduced and their accuracy are shown in Table 7. The fitness function is computed as:

$$fitnessfunction = \alpha * error + \beta * (num - features/maxfeatures) \tag{3}$$

Eq. (4) [39] is designed to make the start-to-contraction mode model the approaching method of slime mold in the mathematical model of SMA.

$$x_{t+1} = \begin{cases} X_b(t) + V_b(W.X_A(t) - X_B(t)) & : x < p \\ V_c.X_t & : x \geq p \end{cases} \tag{4}$$

where x_b is a parameter with an interval [-a, a], V_c falls from one to zero linearly, t represents the current version, X_b indicates the precise location that has been investigated with the highest order concentration, X is the slime mold location vector, and W is the mass of the slime mold. The weight for each slime mould is computed by

$$W(smallIndex(i)) = \begin{cases} 1 + r.log(\frac{bf-si}{bf-wf} + 1)condition \\ 1 - r.log(\frac{bf-si}{bf-wf} + 1)others \end{cases} \tag{5}$$

P is computed as [39]:

$$p = \tan|S_i - DF| \tag{6}$$

where S_i is the fitness of X, and DF is, throughout every iteration, the most fit. The following is an updated mathematical rule for the location of slime mold [40]

$$X^* = \begin{cases} rand(UB - LB) + LB & : rand < z \\ X_b(t) + V_b(WX_A(t) - X_B(t)) & : x < p \\ V_cX(t) & : X \geq p \end{cases} \tag{7}$$

The SMA parameter values are presented in **Table 3**. Setting up parameters and values of the used SMA., while its workflow is illustrated in Figure 5 [41] and its algorithm is presented in Algorithm 1.

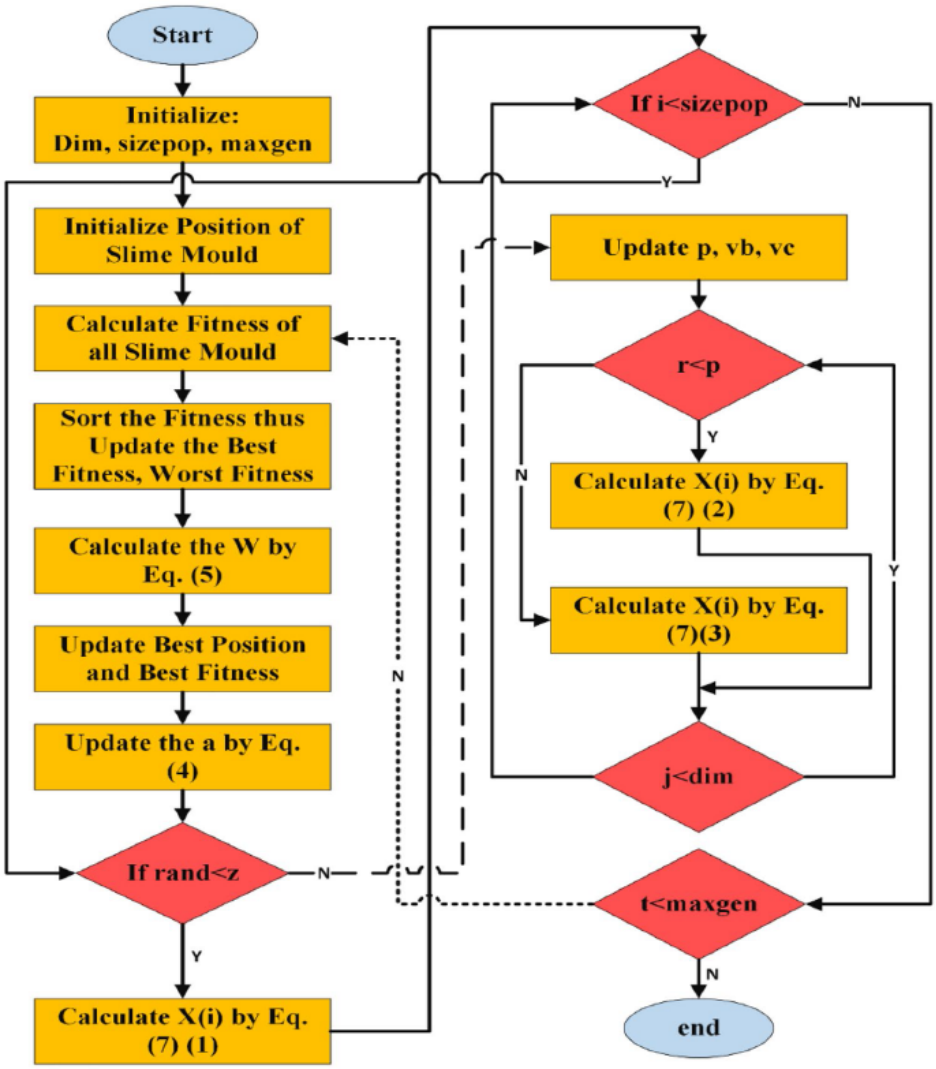

Figure 5. The flowchart of the SMA feature selection algorithm

Algorithm 1: Slime Mould Algorithm

Input: Population Size, MaxIters, Z

Output: selected feature to train classification step

Initialize of variable: initialize slime mould position, Xi|i=1, 2…… Population Size; t←0

While t< MaxIters do

Calculate fitness function using Eq 3

Update the best fitness,

Calculate Weight W

a← $a \tanh \left(1 - \frac{t}{MaxIters}\right)$

b ,$(1 - \frac{t}{MaxIters})$

AgentIndex ←0

While AgentIndex< Population Size do

Update p, using Eq 5,6

Update Mould position using Eq 7

AgentIndex←AgentIndex +1

End While

End while

3.2.5 Classification Stage

Sorting the best-selected features into categories is the main objective of this step. In this step, KNN, ResNet 18, and Fine Gaussian SVM (FGSVM) are utilized. For classification and regression, a non-parametric supervised method called the KNN is applied. It stores all the current data and classifies newly collected data according to similarity [42].

ResNet18 is made up of several layers as shown in Figure 6 [43] , with max pooling being used to transform the final average pooling layer. The final max pooling layer aids in the extraction of the deep features. The first layer of ResNet18, a 7x7 kernel, requires images with an input size of 224*224*3. ResNet18 has eight layers in total. Four comparable ConvNets layers are shown in Figure 7 [44]. Each of these layers' two residual blocks, which consist of two weight layers and a RELU, has a skip link that connects to the output of the second weight layer. Using a pattern, SVM is a

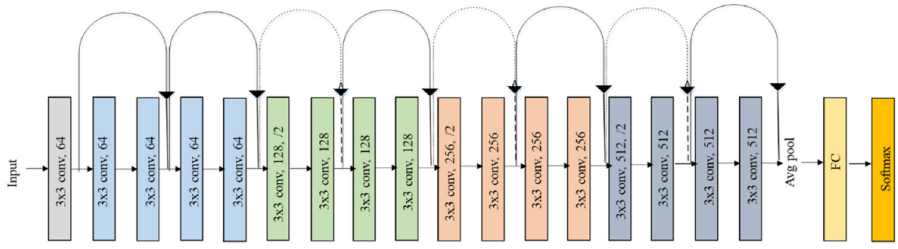

Figure 6. The architecture of ResNet-18

supervised learning technique that can be recognized. The best hyperplane with the biggest margin between two classes is found using this method [45]. SVM uses a variety of kernels, including Gaussian, polynomial, and linear. ResNet 18 is the most suitable ML algorithm for this step. As was covered in the preceding part, the model is first trained using the dataset of CT images. The employed algorithms are trained on 70% of the dataset, with the remaining portion being used for testing. ResNet 18 is a successful classifier as a result. Its accuracy, sensitivity, and specificity are well-balanced. In this stage, there are two classes either malignant or benign. The framework of our

Layer Name	Output Size	18-Layer
Conv1	112*112	
Conv 2_x	56*56	$\begin{bmatrix} 3*3,64 \\ 3*3,64 \end{bmatrix} \times 2$
Conv 3_x	28*28	$\begin{bmatrix} 3*3,128 \\ 3*3,128 \end{bmatrix} \times 2$
Conv 4_x	14*14	$\begin{bmatrix} 3*3,256 \\ 3*3,256 \end{bmatrix} \times 2$
Conv 5_x	7*7	$\begin{bmatrix} 3*3,512 \\ 3*3,512 \end{bmatrix} \times 2$
	1*1	
FlOPs		$1.8*10^9$

Basic Block

Number of times to repeat basic block

Figure 7. The convolution layer in ResNet 18

steps in detail is shown in Figure8.

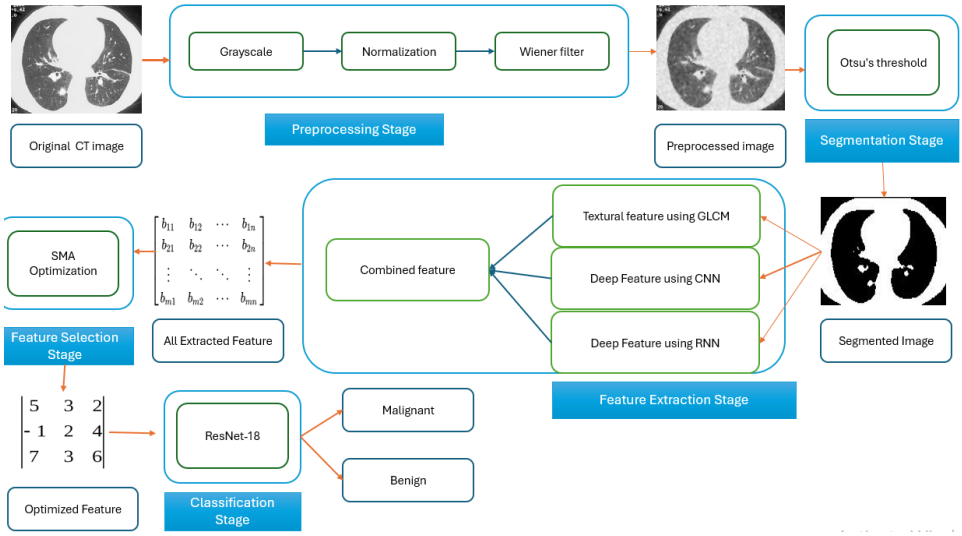

Figure 8. The detailed steps of the Proposed Framework

4. Evaluation

In this work, a computer equipped with a 2.7 GHz Intel R Core (TM) i7-6820HQ CPU, 16 GB of RAM, and MATLAB R 2021 was used to conduct the experimentation on 100 CT image samples from the LIDC-IDRI dataset [31] is used in the conducted experimentation.

4.1 The Evaluation Metrics

To evaluate the effectiveness of the suggested method, three main analytical criteria are employed: accuracy, sensitivity, and specificity. The total number of successfully classified segmented photos of True Positives is known as True Positive (TP). The total number of segmented true negative photographs that are wrongly identified is called True Negative (TN). The False Positive Rate (FPR) is the proportion of improperly segmented images that are correctly classified.

1. Accuracy

$$Accuracy = \frac{Tp + Tn}{Tp + Tn + Fp + Fn} \tag{8}$$

Compared to the other techniques under comparison, the suggested technique detects lung cancer with a 98.5% accuracy rate.

2. Sensitivity A system's sensitivity is determined by how well it can identify true positives. It has the following definition:

$$Sensitivity = \frac{Tp}{Tp + Fn} \tag{9}$$

The suggested method obtains 98.5%, indicating that lung cancer (malignant) on CT scans of the lungs can be accurately identified.

3. Specificity Accurate negatives are what a system can identify with specificity. Its definition is:

$$Specificity = \frac{Tn}{Tn + Fn} \tag{10}$$

With a 99.5 % accuracy rate, the suggested method can accurately identify benign lung cancer in CT scans of the lungs.

4.2 Feature Extraction Comparison

Table 3 demonstrates the comparison of the used feature extraction methods by applying GLCM and hybrid CNN and RNN using three classifiers: KNN, Fine Gaussian SVM (FGSVM), and Resnet-18 is performed.

Table 3. Comparison of feature extraction methods

Classifier	Accuracy	Sensitivity	Specificity
ResNet-18	98.5	98	99.5
KNN	86.7	87.5	90.6
FGSVM	93.5	92.5	95.5

4.3 Feature Selection Comparison

Table 5 and Figure10 show how the wrapper technique in the fitness function, which depends on the KNN algorithm with an accuracy criterion, compares to the employed PSO, SMA, and WOA optimizers. Tables 2, 3, and 4 give the PSO, SMA, and WOA values and setup settings, respectively.

Table 4. Setting up parameters and values of the used PSO

Algorithm	Paramters	Values
PSO	Lb	0
	Ub	1
	thresh	0.5
	c1	2
	c2	2
	W	0.9

Table 5. Setting up parameters and values of the used SMA

Algorithm	Paramters	Values
SMA	Lb	0
	Ub	1
	thresh	0.5
	Z	0.03

Table 6. Setting up parameters and values of the used WOA

Algorithm	Paramters	Values
WOA	Lb	0
	Ub	1
	thresh	0.5
	B	1

Table 7. Comparisons between PSO, SMA, and WOA algorithms with accuracy criterion

Algithms	The number of feature reduces	Accuracy
PSO	198	86.6
SMA	105	95
WOA	135	92.5

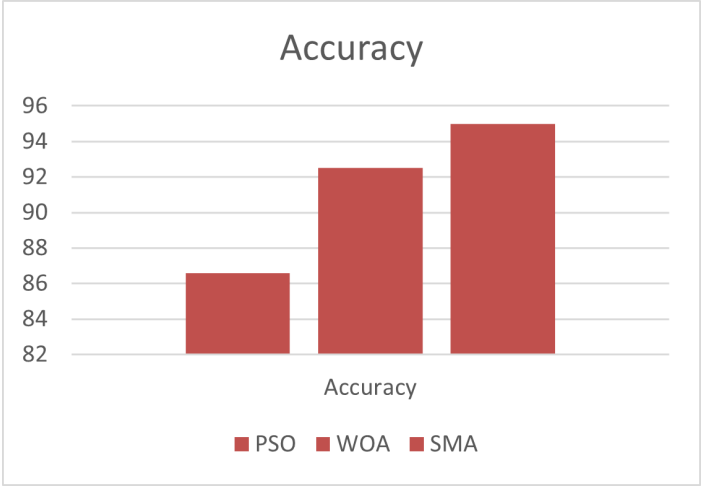

Figure 9. PSO, WOA, and SMA accuracy comparison.

4.4 Classification Methods Comparison

A comparison of ResNet 18, KNN, and FGSVM-trained classification models is performed on three different feature selection algorithms. The optimization algorithms used in the features selection stage are PSO, SMA, and WOA, while the feature extraction methods are GLCM, CNNRNN, or both. The result of the pre-trained network with different feature extraction and different optimizers is

shown in **Table 8** , **Table9** , and **Table 10** . As shown in Table 8 , the best classification algorithm is ResNet 18, and the best feature extraction algorithm is GLCM with CNNRNN.
From Table 8,9,10 , we see that in all three classifiers, the best result is in combining GLCM which provides textural features with CNNRNN providing deep features. In the whole above table, we get the best results by using the ResNet-18 classifier with GLCM and CNNRNN for extracting features.

Table 8. A comparison of a pre-trained network of different features based on using PSO

System with Features		Accuracy	Sensitivity	Specificity
ResNet18	GLCM	85	92	94
	CNNRNN	88.6	94.3	96
	GLCM and CNNRNN	**96.5**	**98.5**	**99.5**
FGSVM	GLCM	87	93	95
	CNNRNN	94.3	100	98
	GLCM and CNNRNN	**95.5**	**98**	**99.5**
KNN	GLCM	86.6	92	94
	CNNRNN	90.5	93.2	97.3
	GLCM and CNNRNN	**93.3**	**95.6**	**97.3**

Table 9. A comparison of a pre-trained network of different features based on using SMA

System with Features		Accuracy	Sensitivity	Specificity
ResNet18	GLCM	73.3	84.6	88.3
	CNNRNN	80.5	86.5	89.5
	GLCM and CNNRNN	**98.5**	**98.5**	**99.5**
FGSVM	GLCM	86.7	90.5	92.7
	CNNRNN	90.4	94.2	96.4
	GLCM and CNNRNN	**96.7**	**98.3**	**98.6**
KNN	GLCM	80	84.6	92.4
	CNNRNN	81.4	85.2	87.4
	GLCM and CNNRNN	**84.5**	**87.5**	**89.5**

Table 10. A comparison of a pre-trained network of different features based on using WOA

System with Features		Accuracy	Sensitivity	Specificity
ResNet18	GLCM	73.3	82.3	86.6
	CNNRNN	90.5	91.5	94.5
	GLCM and CNNRNN	**92.3**	**94.5**	**96.3**
FGSVM	GLCM	86.7	90.5	91.7
	CNNRNN	86.6	89.3	92.6
	GLCM and CNNRNN	**94.2**	**95.4**	**97.4**
KNN	GLCM	80.3	84.3	87.6
	CNNRNN	82.9	86.3	89.9
	GLCM and CNNRNN	**87.6**	**89.3**	**92.6**

4.5 Applying the Proposed Techniques based on using SMA and ResNet

The results of the proposed technique using SMA optimizer and ResNet 18 classifier for the (LIDC-IDRI) Dataset, are shown in Figure 11 below, where **(a)** is the original CT scan from the dataset. **(b)** is the preprocessed Picture, and the segmented image is given in **(c)**.

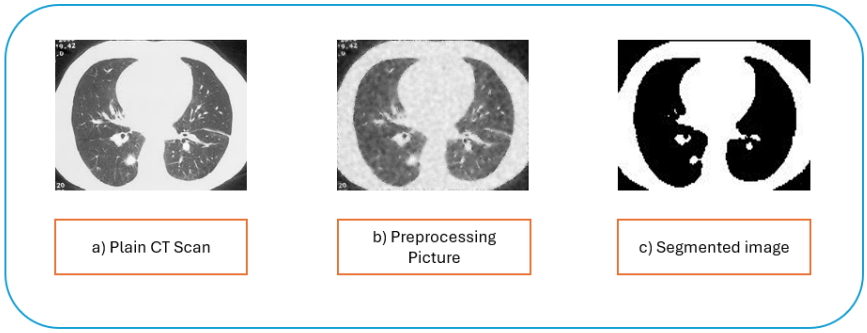

Figure 10. The results of the proposed technique

4.6 Discussion

Table11 demonstrates the effectiveness of the recommended method and a few cutting-edge systems using the LIDC-IDRI dataset. This table shows that our proposed technique has a higher accuracy. Also, this table shows that the work in [3] has better sensitivity and specificity than the proposed technique; however, the system in [3] endure this suffering. There are no documented juxta-pleural, well-circumscribed, vascularized, or pleural tail nodes. Consequently, this research offers an improved technique for identifying lung cancer and determining whether it is benign or malignant. The work shows that the suggested model has some limitations, not simply a stage, but also classifying the cancer as a benign or malignant tumor. Therefore, we want to use different datasets for training and testing this method in the future, as well as different feature extraction and optimization strategies.

Table 11. The Evaluation of the performance of some state-of-the-art systems based and the (LIDC-IDRI) dataset.

System	Year	Accuracy	Sensitivity	Specificity
[3]	2021	96%	99	100%
[27]	2020	92.63%	90.7%	93.47%
[29]	2019	96.7%	-	-
[30]	2023	95%	87%	90%
The proposed technique	2024	98.5%	98.5%	99.5%

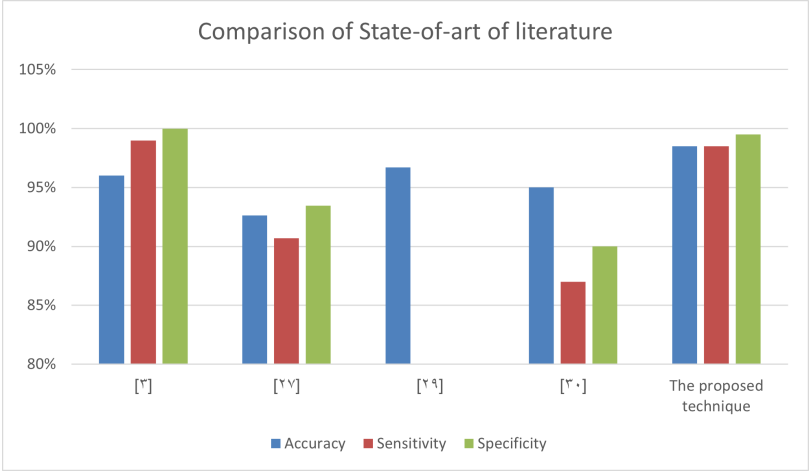

Figure 11. Comparison of State-of-art of literature

5. Conclusion

Lung cancer is one of the most dangerous types of cancer in the world. It is therefore necessary to discover it early. Here in the research, we are discussing a new technique for detecting lung cancer. This technique consists of five steps, which involve preprocessing CT images using a wiener filter which improves the image by reducing noise. Then, feature extraction which combines textural features, and deep features. Textural features are extracted from the GLCM method and deep features from CNN and RNN. These features are combined to improve the accuracy of lung cancer identification. Following this phase, We applied three optimization algorithms to select the best features and compared the results of them. The best optimization algorithm is SMA With a 95% accuracy rate. To identify normal and abnormal lung CT visuals, three classifiers—ResNet 18, FGSVM, and KNN—are used.The best classifier is ResNet-18 of all three classifiers. The accuracy of the newly introduced method is 98.5% accuracy, 98.5 % Sensitivity, and 99.5 % specificity. In future work, we plan to employ a variety of feature selection techniques to determine which technique produces the best results in terms of classification and tumor segmentation accuracy and efficiency. Ultimately, a range of feature extraction and classification techniques will be applied to assess the system's performance.

Open data statement

This paper used the Lung Image Database Consortium Image Collection (LIDC-IDRI) which is available at https://www.cancerimagingarchive.net/collection/lidc-idri/. This dataset includes 1018 images of malignant and healthy tissue.

References

[1] "World Health Organization (2019, 9/4/2019) Cancer fact sheet". In: *URL https:// www.who.int/en/news-room/fact-sheets/detail/cancer'* ().

[2] Dayong Wang, Aditya Khosla, Rishab Gargeya, Humayun Irshad, and Andrew H Beck. "Deep learning for identifying metastatic breast cancer". In: *arXiv preprint arXiv:1606.05718* (2016).

[3] J Prasad, S Chakravarty, and M Vamsi Krishna. "Lung cancer detection using an integration of fuzzy K-means clustering and deep learning techniques for CT lung images". In: *Bulletin of the Polish Academy of Sciences Technical Sciences* (2022), e139006–e139006.

[4] Rahat Idrees, M Abid, Saleem Raza, Muhammad Kashif, Muhammad Waqas, Mubashir Ali, and Laiba Rehman. "Lung cancer detection using supervised machine learning techniques". In: (2022).

[5] Serhat Ozekes, Onur Osman, and Osman N Ucan. "Nodule detection in a lung region that's segmented with using genetic cellular neural networks and 3D template matching with fuzzy rule based thresholding". In: *Korean journal of radiology* 9.1 (2008), pp. 1–9.

[6] Rabia Bashir, Riaz Junejo, Nadia N Qadri, Martin Fleury, and Muhammad Yasir Qadri. "SWT and PCA image fusion methods for multi-modal imagery". In: *Multimedia tools and applications* 78 (2019), pp. 1235–1263.

[7] Imran Nazir, Ihsan ul Haq, Salman A AlQahtani, Muhammad Mohsin Jadoon, and Mostafa Dahshan. "Machine Learning-Based Lung Cancer Detection Using Multiview Image Registration and Fusion". In: *Journal of Sensors* 2023.1 (2023), p. 6683438.

[8] Shidan Wang, Donghan M Yang, Ruichen Rong, Xiaowei Zhan, Junya Fujimoto, Hongyu Liu, John Minna, Ignacio Ivan Wistuba, Yang Xie, and Guanghua Xiao. "Artificial intelligence in lung cancer pathology image analysis". In: *Cancers* 11.11 (2019), p. 1673.

[9] SanaUllah Khan, Naveed Islam, Zahoor Jan, Ikram Ud Din, and Joel JP C Rodrigues. "A novel deep learning based framework for the detection and classification of breast cancer using transfer learning". In: *Pattern Recognition Letters* 125 (2019), pp. 1–6.

[10] Francisco Silva, Tania Pereira, Ines Neves, Joana Morgado, Claudia Freitas, Mafalda Malafaia, Joana Sousa, João Fonseca, Eduardo Negrão, Beatriz Flor de Lima, et al. "Towards machine learning-aided lung cancer clinical routines: Approaches and open challenges". In: *Journal of Personalized Medicine* 12.3 (2022), p. 480.

[11] Ahmed A Alsheikhy, Yahia Said, Tawfeeq Shawly, A Khuzaim Alzahrani, and Husam Lahza. "A CAD system for lung cancer detection using hybrid deep learning techniques". In: *Diagnostics* 13.6 (2023), p. 1174.

[12] Nuruzzaman Faruqui, Mohammad Abu Yousuf, Md Whaiduzzaman, AKM Azad, Alistair Barros, and Mohammad Ali Moni. "LungNet: A hybrid deep-CNN model for lung cancer diagnosis using CT and wearable sensor-based medical IoT data". In: *Computers in Biology and Medicine* 139 (2021), p. 104961.

[13] Akitoshi Shimazaki, Daiju Ueda, Antoine Choppin, Akira Yamamoto, Takashi Honjo, Yuki Shimahara, and Yukio Miki. "Deep learning-based algorithm for lung cancer detection on chest radiographs using the segmentation method". In: *Scientific Reports* 12.1 (2022), p. 727.

[14] M Rashidul Hasan and Muntasir Al Kabir. "Lung cancer detection and classification based on image processing and statistical learning". In: *Journal of Emerging Trends in Engineering and Applied Sciences* 11.6 (2020), pp. 229–236.

[15] Monika Bansal, Munish Kumar, Monika Sachdeva, and Ajay Mittal. "Transfer learning for image classification using VGG19: Caltech-101 image data set". In: *Journal of ambient intelligence and humanized computing* (2023), pp. 1–12.

[16] Mesut Toğaçar. "Disease type detection in lung and colon cancer images using the complement approach of inefficient sets". In: *Computers in Biology and Medicine* 137 (2021), p. 104827.

[17] Md Alamin Talukder, Md Manowarul Islam, Md Ashraf Uddin, Arnisha Akhter, Khondokar Fida Hasan, and Mohammad Ali Moni. "Machine learning-based lung and colon cancer detection using deep feature extraction and ensemble learning". In: *Expert Systems with Applications* 205 (2022), p. 117695.

[18] Mamoona Humayun, R Sujatha, Saleh Naif Almuayqil, and NZ Jhanjhi. "A transfer learning approach with a convolutional neural network for the classification of lung carcinoma". In: *Healthcare*. Vol. 10. 6. MDPI. 2022, p. 1058.

[19] Aiden Nibali, Zhen He, and Dennis Wollersheim. "Pulmonary nodule classification with deep residual networks". In: *International journal of computer assisted radiology and surgery* 12 (2017), pp. 1799–1808.

[20] Ahmed Shaffie, Ahmed Soliman, Luay Fraiwan, Mohammed Ghazal, Fatma Taher, Neal Dunlap, Brian Wang, Victor van Berkel, Robert Keynton, Adel Elmaghraby, et al. "A generalized deep learning-based diagnostic system for early diagnosis of various types of pulmonary nodules". In: *Technology in cancer research & treatment* 17 (2018), p. 1533033818798800.

[21] S Shanthi and N Rajkumar. "Lung cancer prediction using stochastic diffusion search (SDS) based feature selection and machine learning methods". In: *Neural Processing Letters* 53.4 (2021), pp. 2617–2630.

[22] K Punithavathy, MM Ramya, and Sumathi Poobal. "Analysis of statistical texture features for automatic lung cancer detection in PET/CT images". In: *2015 International Conference on Robotics, Automation, Control and Embedded Systems (RACE)*. IEEE. 2015, pp. 1–5.

[23] Mesut Toğaçar, Burhan Ergen, and Zafer Cömert. "Detection of lung cancer on chest CT images using minimum redundancy maximum relevance feature selection method with convolutional neural networks". In: *Biocybernetics and Biomedical Engineering* 40.1 (2020), pp. 23–39.

[24] Anum Masood, Bin Sheng, Ping Li, Xuhong Hou, Xiaoer Wei, Jing Qin, and Dagan Feng. "Computer-assisted decision support system in pulmonary cancer detection and stage classification on CT images". In: *Journal of biomedical informatics* 79 (2018), pp. 117–128.

[25] Surbhi Vijh, Prashant Gaurav, and Hari Mohan Pandey. "Hybrid bio-inspired algorithm and convolutional neural network for automatic lung tumor detection". In: *Neural Computing and Applications* 35.33 (2023), pp. 23711–23724.

[26] Mustafa Ghaderzadeh, Farkhondeh Asadi, Ramezan Jafari, Davood Bashash, Hassan Abolghasemi, and Mehrad Aria. "Deep convolutional neural network–based computer-aided detection system for COVID-19 using multiple lung scans: design and implementation study". In: *Journal of Medical Internet Research* 23.4 (2021), e27468.

[27] Antonio Oseas de Carvalho Filho, Aristofanes Corrêa Silva, Anselmo Cardoso de Paiva, Rodolfo Acatauassú Nunes, and Marcelo Gattass. "Classification of patterns of benignity and malignancy based on CT using topology-based phylogenetic diversity index and convolutional neural network". In: *Pattern Recognition* 81 (2018), pp. 200–212.

[28] Guohui Wei, He Ma, Wei Qian, Fangfang Han, Hongyang Jiang, Shouliang Qi, and Min Qiu. "Lung nodule classification using local kernel regression models with out-of-sample extension". In: *Biomedical Signal Processing and Control* 40 (2018), pp. 1–9.

[29] R Ankita, Ch Usha Kumari, Mohd Javeed Mehdi, N Tejashwini, and T Pavani. "Lung cancer image-feature extraction and classification using GLCM and SVM classifier". In: *Int. J. Innov. Technol. Explor. Eng* 8.11 (2019), pp. 2211–2215.

[30] Shalini Wankhade and S Vigneshwari. "A novel hybrid deep learning method for early detection of lung cancer using neural networks". In: *Healthcare Analytics* 3 (2023), p. 100195.

[31] Temesguen Messay, Russell C Hardie, and Timothy R Tuinstra. "Segmentation of pulmonary nodules in computed tomography using a regression neural network approach and its application to the lung image database consortium and image database resource initiative dataset". In: *Medical image analysis* 22.1 (2015), pp. 48–62.

[32] Mehmet Sezgin and Bulent Sankur. "Survey over image thresholding techniques and quantitative performance evaluation". In: *Journal of Electronic imaging* 13.1 (2004), pp. 146–168.

[33] Zewen Li, Fan Liu, Wenjie Yang, Shouheng Peng, and Jun Zhou. "A survey of convolutional neural networks: analysis, applications, and prospects". In: *IEEE transactions on neural networks and learning systems* 33.12 (2021), pp. 6999–7019.

[34] Sakorn Mekruksavanich and Anuchit Jitpattanakul. "Deep convolutional neural network with rnns for complex activity recognition using wrist-worn wearable sensor data". In: *Electronics* 10.14 (2021), p. 1685.

[35] Wenjie Lu, Jiazheng Li, Jingyang Wang, and Lele Qin. "A CNN-BiLSTM-AM method for stock price prediction". In: *Neural Computing and Applications* 33.10 (2021), pp. 4741–4753.

[36] Walid Al-Dhabyani, Mohammed Gomaa, Hussien Khaled, and Fahmy Aly. "Deep learning approaches for data augmentation and classification of breast masses using ultrasound images". In: *Int. J. Adv. Comput. Sci. Appl* 10.5 (2019), pp. 1–11.

[37] Bo Zhao, Jiashi Feng, Xiao Wu, and Shuicheng Yan. "A survey on deep learning-based fine-grained object classification and semantic segmentation". In: *International Journal of Automation and Computing* 14.2 (2017), pp. 119–135.

[38] Greg Van Houdt, Carlos Mosquera, and Gonzalo Nápoles. "A review on the long short-term memory model". In: *Artificial Intelligence Review* 53.8 (2020), pp. 5929–5955.

[39] T Ibrikci FS Gharehchopogh A Ucan and G Isik B Arasteh. "Slime Mould Algorithm: A Comprehensive Survey of Its Variants and Applications". In: *Archives of Computational Methods in Engineering* 60.4 (2023), pp. 2683–2723.

[40] KM Daud Y Wei Z Othman and Y Zhou Q Luo. "Advances in Slime Mould Algorithm: A Comprehensive Survey". In: *Biomimetics* (2024).

[41] BP Soni A Singh A Saxena. "Comparison of Population-Based Intelligent Techniques to Solve Load Dispatch Problem". In: *European Journal of Advances in Engineering and Technology* (2015).

[42] H Wang G Guo and K Greer D Bell Y Bi. "KNN Model-Based Approach in Classification". In: *In On The Move to Meaningful Internet Systems 2003* (2003).

[43] A Rehmat F Ramzan MUG Khan, T Saba S Iqbal, and Z Mehmood A Rehman. "A Deep Learning Approach for Automated Diagnosis and Multi-Class Classification of Alzheimer's Disease Stages Using Resting-State fMRI and Residual Neural Networks". In: *Journal of medical systems* (2020).

[44] W Qian W Sun B Zheng. "Computer aided lung cancer diagnosis with deep learning algorithms". In: *Medical imaging* (2016).

[45] B Lekha KS Durgesh. "Data classification using support vector machine". In: *Journal of theoretical and applied information technology* (2010).